Determination of the hydrodynamic parameters of two types of soil in the Senegal River delta. Simulation of hydro-saline transfers: application to the wind deflation phenomenon

Fary Diome[1], Landing Biaye[2]*

[1&2] *Institute of Earth Sciences, Faculty of Science and Technology, B. P. 5396, Dakar-Fann Senegal*

Authors LB and FD designed the study, performed the statistical analysis. Author LB made the maps. Author FD wrote the protocol and wrote the first draft of the manuscript. Author LB manage the analyses of the samples. Authors LB, FD and MM managed the literature searches. All authors read and approved the final manuscript.

ABSTRACT

In the Senegal River delta, the presence of a shallow salt water table associated with a strong evaporative demand sometimes leads to an upwelling of salts that crystallize on the surface. This phenomenon can be observed in the vicinity of the Diawling Basin, where a powdery structure sensitive to wind deflation and a massive structure with a fractionation into platelets that cannot be transported by the wind are noted.

To understand the hydrodynamic characteristics of these soils, we used numerical simulation of water and solute transfers. The hydrodynamic parameters were determined in the laboratory using Wind's method on undisturbed samples. The experimental retention h() and hydraulic conductivity K(h) curves were fitted using the Van Genuchten model. The simulations show that the soil with a powdery structure has hydrodynamic characteristics that favour the ascent of salts from the water table to the surface. For the soil with a massive structure, the hydrodynamic conditions impose a deposition of salts in the subsurface.

Keywords *: a salty tablecloth ; Wind method ; hydrodynamic parameters ; wind deflation ; soil.*

1. INTRODUCTION

The high evaporative demand that characterizes arid and semi-arid zones leads to a concentration of surface water and a precipitation of salts that will accumulate over time. This accumulation leads to three types of saline degradation: salinisation, sodisation and alkalinisation. These saline degradations destroy the soil structure and make it susceptible to wind erosion; they promote swelling, the dispersion of soil colloids and plant toxicity, and also lead to a reduction in soil fertility. Numerous studies carried out in West Africa mention these problems, particularly those of [1] and Droubi [2] in Chad, [3] and [4] in Mali, [5], [6] in Niger, [7] and [8] in Senegal.

In the Senegal River delta, the saline degradation of soils is at the origin of the wind deflation phenomenon observed in the settling basins ([9]; [10]; [11]; [12]; [13]).

Numerical modelling of hydrosaline transfers is one of the most widely used means to analyse, understand, and consequently prevent these soil degradation mechanisms. In this study, we will experimentally determine the hydrodynamic parameters of two types of soils in the Diawling basin, an area strongly affected by wind deflation in the Senegal River delta.

2. MATERIAL AND METHODS

2.1. Geographical context

Diawling National Park, on the right bank of the Senegal River, is located in Mauritanian territory in the former Senegal River delta plain, about 40 km from the city of Saint-Louis (**Fig. 1**).
The Senegal Delta is located in the Sahelo-Saharan climatic zone, characterized by the alternation of a rainy season and a dry season.
The rainy season is short (July and August) and rainfall is low (around 300 mm/year), often irregular and poorly distributed. The dry season is long (from September to June) and characterized by the harmattan, a hot and dry wind that increases evapotranspiration and decreases relative humidity [14].
For the vegetation in Diawling Park, we notice that the lowlands, with the exception of the sebkhas, are covered by a perennial vegetation made up of shrubs (*Acacia nilotica, Indigo fera oblongifolia, Ipomea, Zygophyllum*), grasses of the Sporobolus type and *Tamaris senegalensis*. The dune zones show several species of which the most represented are: *Acacia radiana, Balanites aegyptiaca, Salvadora persica, Acacia albida, Euphorbia balsomifera, Acacia ehrenbegiana, Adonsonia digitata, Zizyphus mauritania, Tamarindus indica* [15].

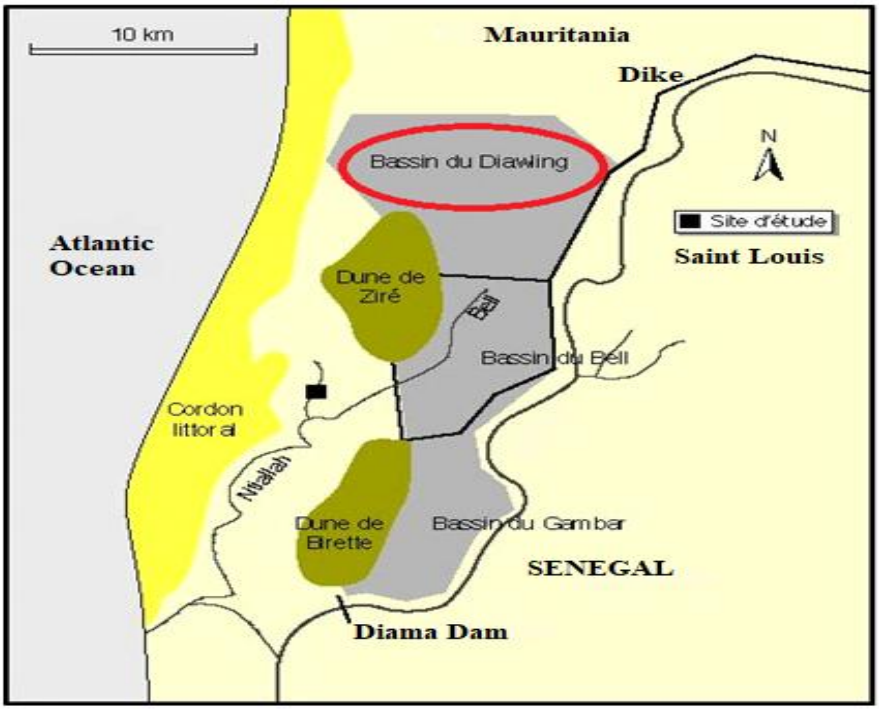

Fig. 1. Location of the profiles on the site

2.2. Geomorphology and Pedology

The geomorphology of the Senegal Valley and Delta is characterized by two clearly defined areas of different ages: the dune model (called "Diéri") resulting from the reworking of the ancient dune massif established during the Ogolian period; and the alluvial plains (called "Oualo") corresponding to the major bed formations established by alluviation of the river, its tributaries and defluents. A cross-section of the valley allows us to distinguish these two large units (**Fig. 2**).

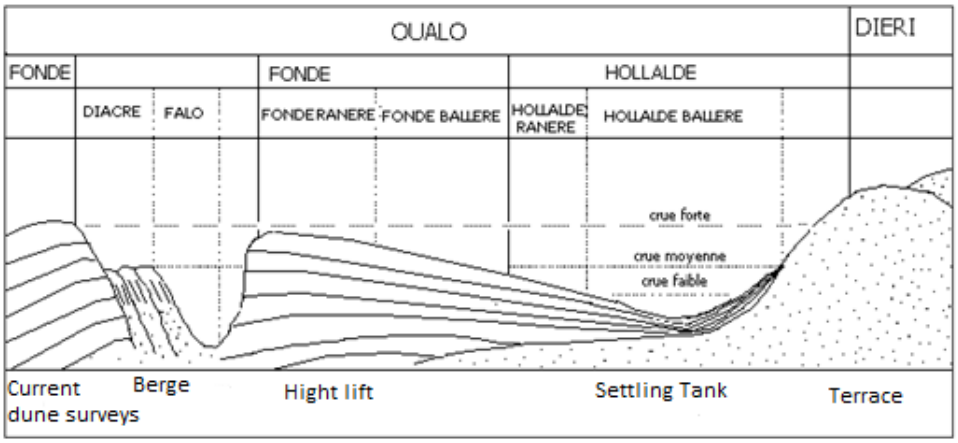

Fig. 2. Schematic section of the Senegal River valley [16]

After the Nouakchottian transgression, the annual floods of the Senegal River built a complex system of river levees:
High levees are made up of light soils called "founded". Small levees include the lowest parts of levee-breaking deltas, the edges of settling basins, and the thin, flattened levees of former tributaries; they cross the basins. The settling basins are often occupied by soils with swelling clays called "hollaldé" and presenting cracks when they are dry. The soils studied were described by [13] who carried out three soil profiles using test pits (**Fig. 3**). One of the soils has a powdery structure sensitive to wind deflation, and the other a massive structure not transportable by the wind.
Profile P1 shows a grey to bluish silty silt with black (pyrite) and yellow (jarosite) tubes. The surface fractionation corresponds to the powdery structure sensitive to wind deflation.
Profile P2 also shows a bluish silt from 55 cm depth with jarosite as before. The powdery structure is found on the surface and the olian deflation is active.
Profile P3 like the first two, also shows a bluish mud but from 85 cm. It is crossed by ochre tubes corresponding to the old mangrove roots. An abrupt transition leads to a sandy material strongly coloured by iron oxides and which can be observed up to 15 cm from the surface. The contour of all volumes is intersected by undulating clay bands of variable thickness (5 to 10 cm).

Fig. 3. Boundary between the two surface states

The wind method
The method of WIND [17] consists of subjecting a cylinder of initially saturated undisturbed soil to progressive drying and following the temporal variation of the soil mass m(t) in the cylinder in order to determine the water loss by evaporation and the evolution of the soil matrix potential h (z, t) as a function of time.

The matrix potential is measured at different depths of the sample using tensiometers. Following a fixed time interval, the weight loss due to water evaporation and the matrix potential are measured and recorded.
The water content of each compartment was estimated from the average water content of the sample and the potential values measured on the tensiometer.
From the potential measurements, h(z,t), and the reconstruction of the water content (z,t), it is possible to draw the retention curve Θ(h) and the hydraulic conductivity curve (K). These curves have been adjusted using mathematical models to determine the hydrodynamic parameters of the soils studied.
The model generally used to fit the retention curve is the Van Genuchten model.

$$S_e = \frac{1}{\left[1+(\alpha h)^n\right]^m}.$$

Considering the expression for Se, the Van Genuchten equation can be written as

$$\theta(h) = \theta_r + (\theta_s - \theta_r)\left[\frac{1}{1+(\alpha h)^n}\right]^m$$

where, **α**, **m** and **n** are constant empirical parameters that determine the shape of the retention curve. Note that :
Θ= Water content by volume of the soil
Θ_r =Residual water content
Θ_s =Saturation water content

2.3. Experimental apparatus

The experimental apparatus includes (**Fig.4**): electronic scales installed in a thermostatically controlled chamber and connected to a computer that displays the weight variations of the samples and voltage sensors that measure the matrix potential at different heights of the soil column.

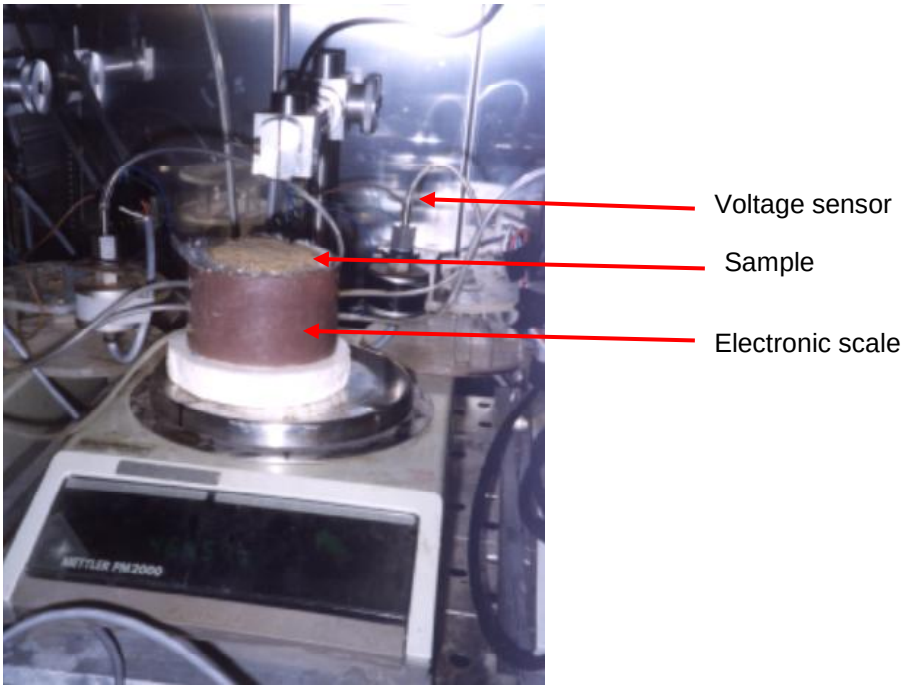

Fig.4. View of the experimental apparatus

2.4. Calibration of sensors

Calibration of the sensors consists of creating a vacuum with a vacuum pump in a mercury manometer and recording the corresponding voltage value. **Table I** gives the different equations obtained for each voltage sensor. **X** will represent depressions in cm of mercury (converted to millibar) and **Y** will be the sensor output voltages in millivolts.

Table I. Calibration equations

Sensors	Calibration equations	Correlation coefficient R^2
C_1	y = - 25,743x + 97,968	0.9999
C_2	y = - 25.919x + 101.7	1
C_3	y = - 26.435x + 100.69	1
C_4	y = - 25.914x + 108.24	1
C_5	y = - 25.549x + 99.1	0.9998
C_6	y = - 25.657x + 97.14	0.9999
C_7	y = - 25,714x + 93,479	0.9999
C_8	y = - 26.34x + 102.79	0.9983

2.5. The experimental protocol

The undisturbed soil samples were collected in 8 cm diameter PVC cylinders which are drilled to allow for the introduction of tensiometers. The interval between samples is electric. By varying the vacuum, a series of data is obtained which allows the characteristic calibration curves of each sensor to be drawn. The distance between two successive holes is constant and is chosen according to the number of tensiometers and the height of the sample.

To avoid air bubbles that could affect the operation of the device, the water introduced into the capillaries is degassed.

2.6. Sample preparation

The samples are dried in an oven at 105°C until their weight stabilizes. They are then introduced into a desiccator to lower the temperature before being weighed to determine their dry weight which will be used in the calculations.

During saturation, the sample is brought into contact at its base with a porous plate placed at the bottom of a tray. It is then subjected to moisture and drying cycles.

After saturation, the samples are weighed again before the tensiometers are inserted. When the tensiometers are inserted, the capillary is filled by sucking out the degassed water with a syringe.

The thermostatic chamber is set at 32°C to ensure correct and gradual drying of the samples.

Weight and blood pressure measurements are taken at 15-minute intervals.

2.7. Data processing

The raw data collected at the end of each run are pre-processed before being entered into the evaluation program. Weight changes due to water evaporation are used to calculate the water content as a function of time for each sample.

Voltage values expressed in millivolts are converted to mbar (or cm of water) using the calibration equations of the corresponding sensors. All these calculations were made using EXCEL software.

3. RESULTS AND DISCUSSION

3.1. EVOLUTION OF TENSIOMETERS

The curves h(t) shown in **figures 5 to 8** show the time evolution of the pressure potential at different depths for each type of sample.

At the beginning of the experiment (t=0), the sample is saturated, the pressure potential h is zero at each tensiometer. As the water evaporates, the pressure potential increases due to the decrease of the water content which is gradually observed from the top to the bottom of the sample. This is reflected in the graphs by the faster growth of one tensiometer compared to the lower one. This difference in the shape of the h(t) curves is clearly visible in the soil with a massive structure (**fig. 5 and 6**).

For the powdery soil (**fig. 7 and 8**), the curves of the three tensiometers are almost merged along the rising part. The top of each curve shows the drop-out of the corresponding monitor.

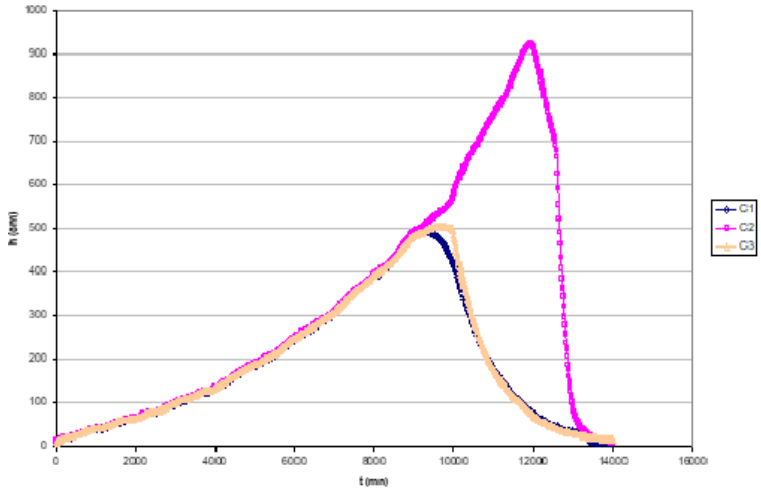

Fig.5. SSM1-Evolution of tensiometers

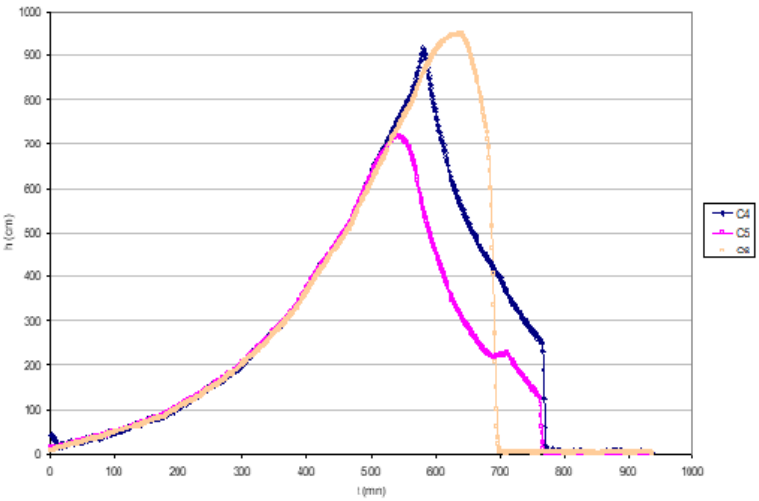

Fig.6. SSM2-Evolution of tensiometers

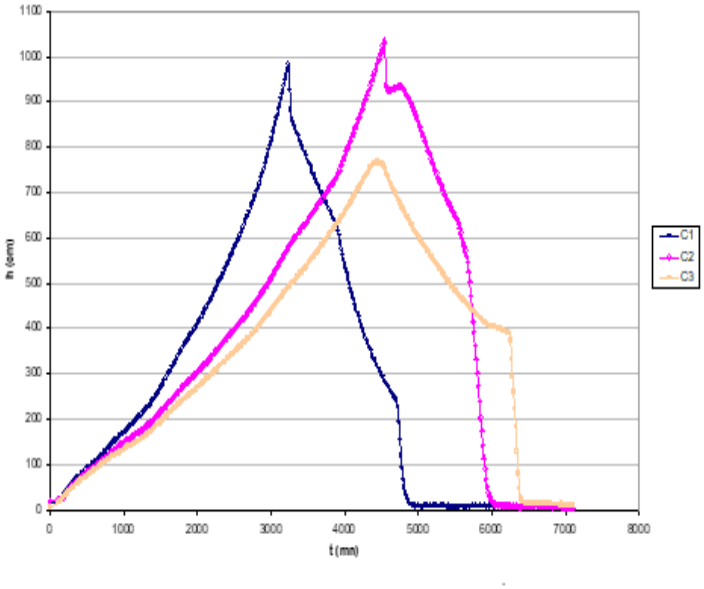

Fig.7. SSP1-Evolution of tensiometers

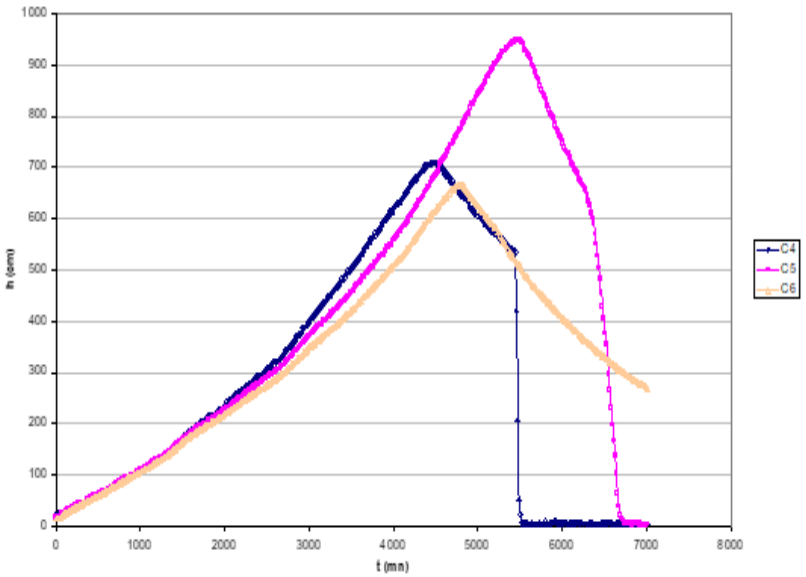

Fig.8. SSP1-Evolution of tensiometers

3.2. ESTABLISHMENT OF THE RETENTION CURVE H ()

The estimation of the hydrodynamic parameters and the fitting of the retention curve were carried out using the empirical Mualem - Van Genuchten model developed in the RETC operating program [18].
This program allows, on the one hand, to plot for each sample the experimental curves and the simulated curves according to a non-linear adjustment method [19]; and on the other hand, the residual water contenter, the saturation water contents, and the coefficients, n and m which can be calculated independently or linked according to the chosen model: m=1-1/n (Van Genuchten - Mualem); m=1-2/n (Van Genuchten - Burdine).
For each tensiometer, the tension (expressed in cm) and the water content are entered into the program as text files (.txt). The curve was adjusted according to the experimental data and the estimated initial values of some parameters that are set at the beginning of the operation.
The experimental and fitted retention curves for the two soil types are shown in **Figures 9** and **10**.
Establishment of the hydraulic conductivity curve k ().
The estimation of the hydraulic conductivity involves the calculation of the instantaneous flows between the different tensiometers. The fitting of the curves was done using the Mualem-Van Genuchten model (with m=1-1/n). We tested the models developed in the RETC code and the Van Genuchten model was chosen because it provided the best fit.
In our study, we were able to fit the K () and h () curves of both samples simultaneously (**Figures 9 and 10**). **Table II** gives the hydrodynamic parameters of the two soils obtained from the experimental data.

Table II. Summary of the hydrodynamic parameters of the two soils

Samples	Compartments	θ_r	θ_s	cm^{-1}	n [-]	l	K_s [cm/d]	Correlation factor
SSM	C1	0	0.31	0.004	1.29	0.5	0.45	0.98
	C2		0.32	0.006	1.25		0.48	0.99
	C3		0.32	0.008	1.18		0.59	0.99
SSP	C1	0.20	0.45	0.016	1.79	-3.70	0.39	0.44
	C2	0.19		0.017	1.71	-3.98	0.27	0.44
	C3	0.19		0.016	1.75	-3.79	0.08	0.47

According to these results, the hydraulic conductivity at saturation is slightly higher for SSM than for SSP, the residual water content is zero for SSM while it is 0.2 for SSP. In addition, a parameter inversely proportional to an average pore size is higher for the SSP than for the SSM. Water transfers are faster in the SSM than in the SSP if only the hydraulic conductivity value at saturation is taken into account. It is noted that during the drying of a saturated soil, the matrix potential increases as a function of the evaporative demand; it is therefore necessary to study the evolution of the hydraulic conductivity as a function of the matrix potential to try to evaluate the fluxes likely to exist in the two types of soil.

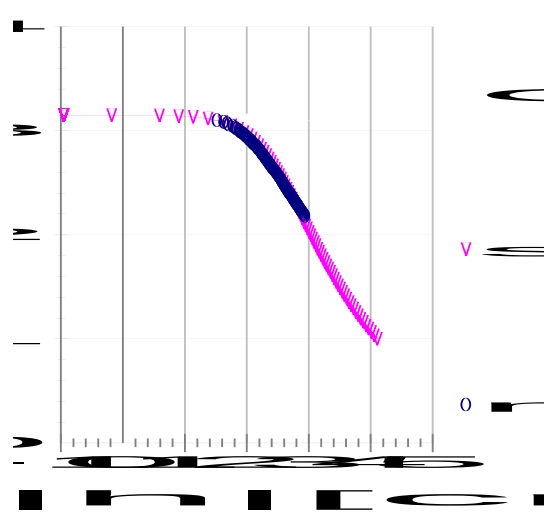

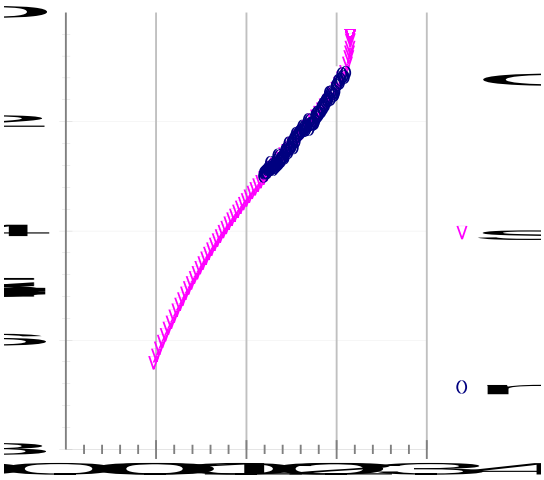

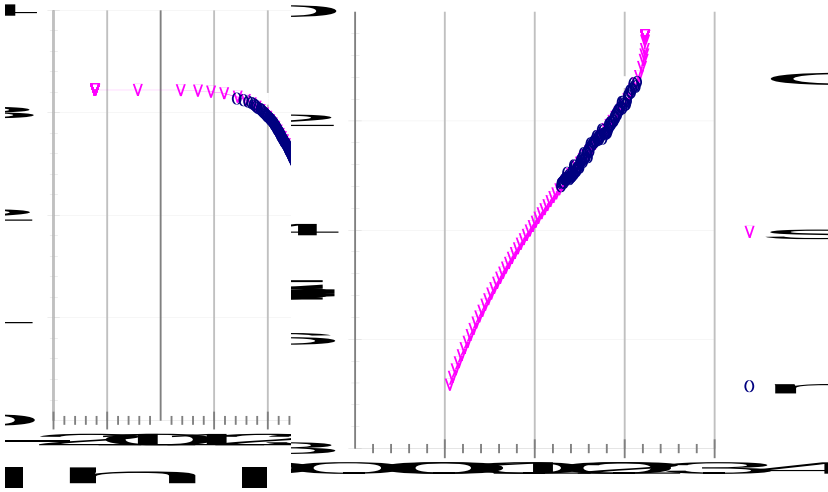

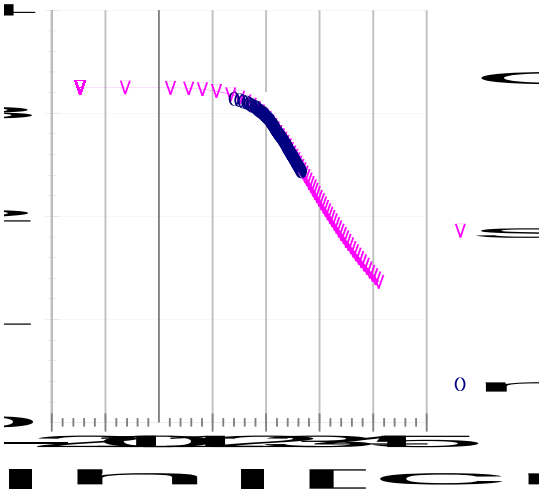

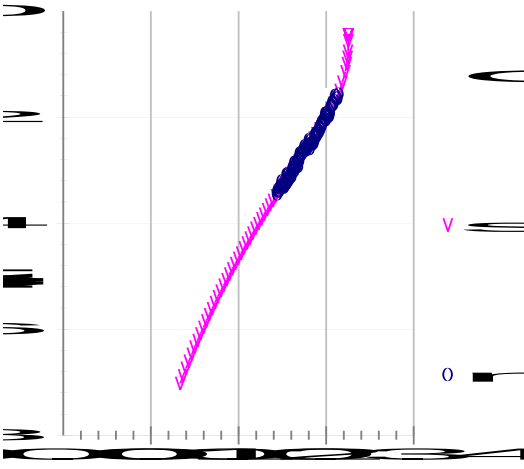

Figure 9. h() and K() curves of the different compartments of the SSM sample fitted to the Van Genuchten - Mualem model (m=1-1/n)

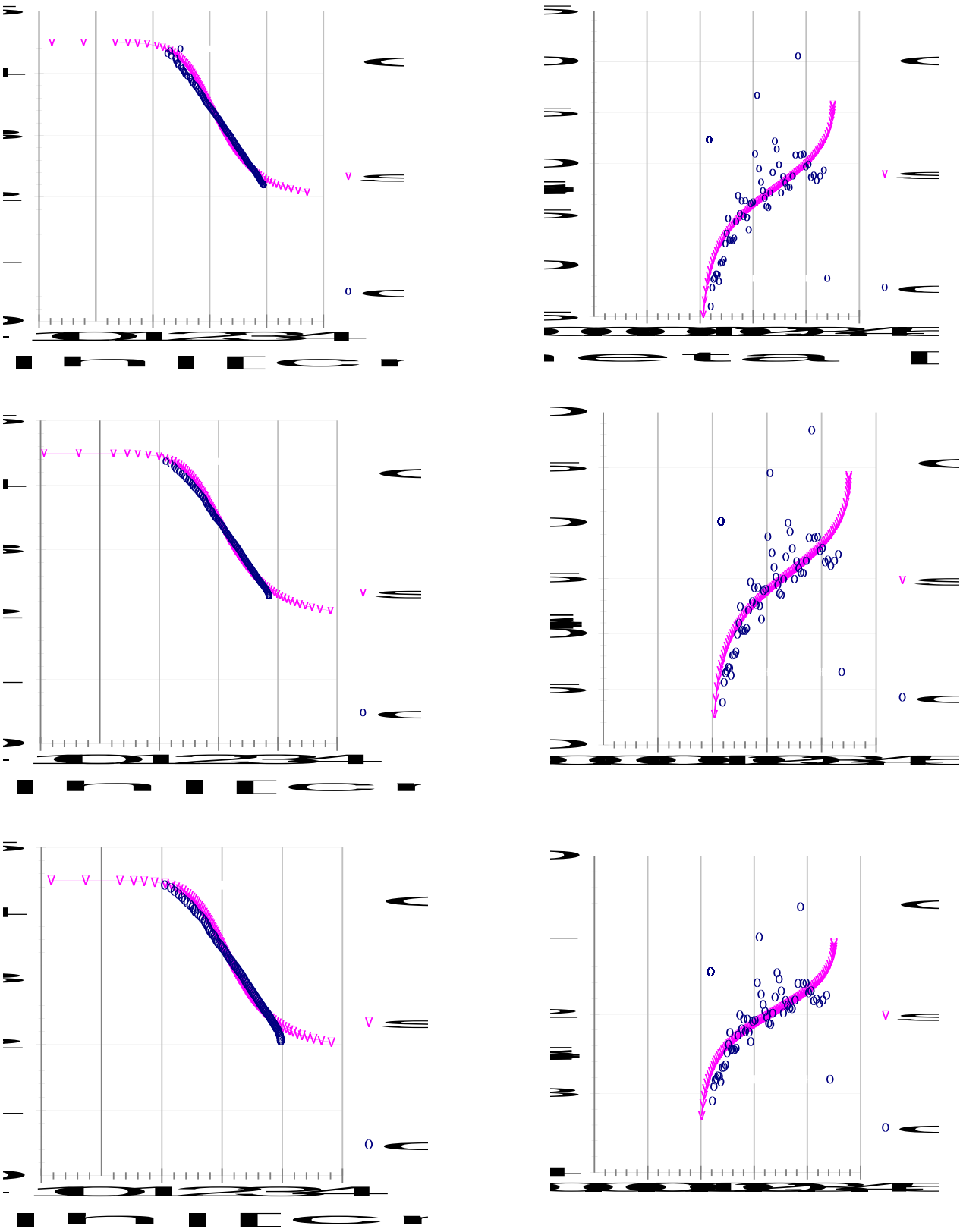

Fig. 10. h() and K() curves of the different compartments of the SSP sample

3.3. Model results

The experimental results allowed this study to determine the hydrodynamic parameters characteristic of the two soils. To better understand their hydrodynamic behaviour, we simulated the evolution of hydraulic conductivity as a function of matrix potential for both types of soil. These curves were obtained from the model proposed by Van Genuchten by integrating the hydrodynamic parameters determined previously.

$$K(\theta) = K_s \left(\frac{\theta - \theta_r}{\theta_s - \theta_r} \right)^{1/2} \left[1 - \left(1 - \left(\frac{\theta - \theta_r}{\theta_s - \theta_r} \right)^{1/m} \right)^m \right]^2$$

The evaporation of water from the soil results in an increase in the matrix potential. At the same time, it leads to a decrease in the hydraulic conductivity of the soil described by the K(h) curve.
The shape of the K(h) curves (**Fig. 11**) shows that the decrease of *K as a* function of evaporation is faster on the SSM than on the SSP. Ah=0 corresponding to the maximum saturation state, the hydraulic conductivity at saturation K_s is greater for the SSM, the K(h) curve of the SSP is below that of the SSM. However, this trend is quickly reversed with increasing h.

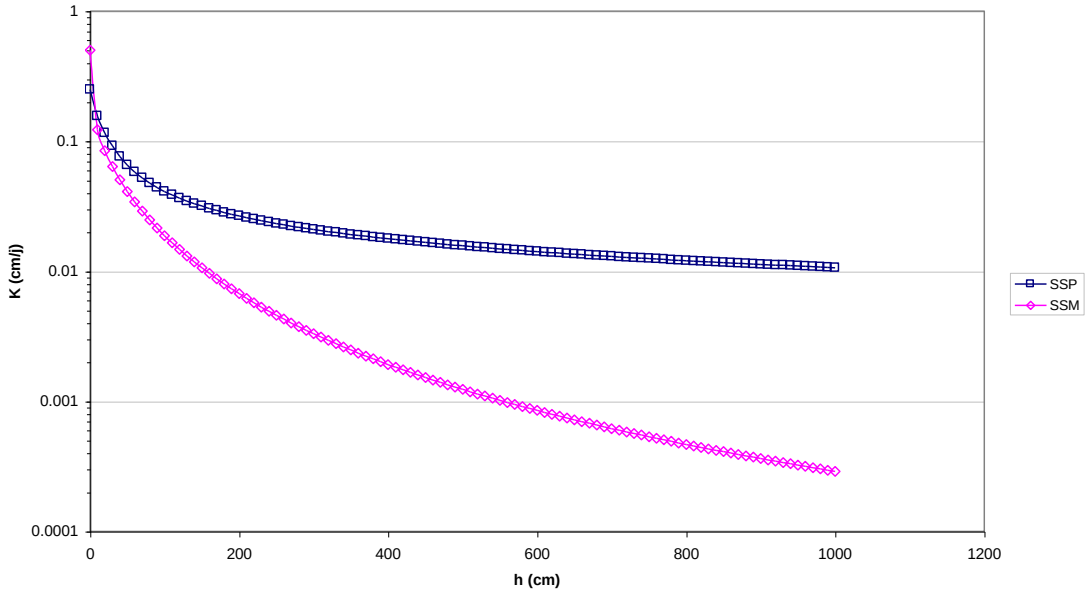

Fig. 11. Comparison of the K(h) curves of the two soils

The h () and K () curves show a difference in behaviour between the two soils. The tensiometers drop out more quickly in the SSM samples, however the variation of the pressure potential with depth is better visualized in these samples where a clear superposition between the evolution curves of the different tensiometers is noted (**Fig. 9 and 10**).
For samples with a powdery structure, the curves of the tensiometers are almost identical.
The fitting of the retention curves allowed a good superposition between the experimental results and those of the model for both samples. However, for the hydraulic conductivity curves, the fit is better for the soil with a massive structure with a correlation coefficient R= 1. It is less good for the soil with a powdery structure with R= 0.4. This difference in behaviour is also reflected in the hydrodynamic parameters. The water content at saturation goes from 0.32 for the soil with massive structure to 0.45 for the soil with powdery structure. Similarly, for this soil, the average hydraulic conductivity at saturation is about 0.3 cm/d, whereas it is about 0.5 cm/d for the soil with a massive structure (**Table n°3**).
The movement of water and solutes in the soil is governed by these parameters, in particular by the hydraulic conductivity.

The analysis of the simulated K(h) curves of the two soils allows a better understanding of their hydrodynamic behaviour. Indeed, the K(h) curves show that the SSM, with a higher Ks, desaturates much faster than the SSP according to the evolution of the matrix pressure potential. Consequently, under the same conditions of pressure potential variation, water containing salt from the water table will reach higher levels in the SSP than in the SSM. The salt can thus reach the upper horizons of the SSP and crystallize at the surface under the effect of evaporation, whereas at the level of the SSM the concentration of salt will be at lower levels in the subsurface. According to the results, it can be said that the SSP soil is more salty on the surface than the SSM soil.

These two soils present a structural difference which is translated on the ground by an abrupt transition of surface state presenting on one side, a powdery structure sensitive to the wind deflation, and on the other side a massive structure with a fractionation in centimetric plates not transportable by the wind [18]. According to [20], the powdery structure is due to the rapid crystallization of salts such as gypsum. At the same time, [21] considers that this structural difference corresponds to a change in texture of the surface horizon, which can be linked to pedogenetic transformations. [22] and [23] consider that this phenomenon is accentuated by the role of wind erosion in the distribution of salts in the Senegal River valley.

On the same site, [9] observed that in the heart of the basins, the more clayey nature of the deposits delays the wind deflation in the season. The same observation was made by [24] and [25] whose work shows that the clay enrichment of the surface horizon blocks the process of crumbling of the surface part of the soil. The flow is no longer in powder but in the form of small centimetric plates, not vulnerable to wind deflation.

4. CONCLUSION

The use of the Van Genuchten model made it possible to obtain a good fit of the retention and hydraulic conductivity curves and thus to determine the characteristic hydrodynamic parameters of the two soils.

The simulation results showed that the solid-structured soil (SSM), which has a higher hydraulic conductivity at saturation than the powdery-structured soil (SSP), desaturates more quickly. The hydrodynamic characteristics of the SSP mean that salt from the water table can reach the upper horizons and crystallize on the surface due to evaporation. The concentration of salt on the surface leads to a destabilization of the soil structure due to the dispersing effect of the sodium contained in the NaCl molecules. The soil then loses its cohesion and becomes sensitive to wind deflation.

At the SSM level, the hydrodynamic characteristics impose a subsurface deposition of salt under the same evaporation conditions.

With the Wind method, all hydrodynamic properties of a soil can be determined simultaneously on a single sample.

REFERENCES

1. Cheverry J. C. Contribution to the pedological study of the polders of Lake Chad. Dynamique des sels en milieu continental subaride dans les sédiments argileux et organiques. 1974 ; Thèse docteur ès Sciences, ULP, Strasbourg, 275 p.
2. Droubi (AI-) A. Geochemistry of salts and concentrated solutions by evaporation. Thermodynamic simulation model. Application aux sols salés du Tchad. 1976 ; Thesis ULP, Strasbourg, Ed. CNRS, 175 p.
3. Ndiaye M. K. Evaluation of soil fertility in the Office du Niger (Mali). Contribution à la recherche des causes et origines de la dégradation des sols dans le Kouroumari. 1987 ; Doct-lng. thesis, INP, Toulouse, 133 p.
4. Valles V., Bertrand R, Bourgeat F. and Ndiaye M. The concept of generalized residual alkalinity and irrigation of sodic soils. Application to the soils of Kouroumari (Mali) and the valley of the oued Medjerdah (Tunisia). 1989 ; Tropical agronomy 44 (3) : 157-163.
5. Barbiero L. and Berrier J. Evidence of a natural dealkalisation of sois in a tropical environment. Transformation of alkaline soils into sub-arid brown soils on a Sahelian lowland in Niger. 1994 ; C. R. Acad. Sci. Paris, 3 19, series II : 659-665.
6. Barbiero L., Valles V. and Regeard A. Precipitation of fluorite and geochemical control of calcium in alkaline soils of Niger. Consequences for a quantitative estimation of soil geochemical evolution.1995 ; C. R. Acad. Sci. Paris, t. 321, series II a : 1147-l 154.

7. Loyer J.Y. Les sols salés de la basse vallée du fleuve Sénégal : caractérisation, distribution et évolution sous cultures. 1989 ; Etudes et Thèses, Ed. ORSTOM, 137 p.
8. Hammecker C. Study of the size distribution of pore accesses by mercury porosimetry on soil columns from Fanaye and Ndiaye.1996 ; Dot. Interne, ORSTOM.
9. Tricart J. Influence of saline soils on aeolian deflation in lower Mauritania and in the Senegal delta. 1954 ; Revue géomorphologie dynamique, 5th year, 3, 123-136.
10. Mougenot B. Characterization and evolution of soil surface conditions in relation to the seasonal dynamics of salts in the Senegal Delta. 1983 ; ORSTOM report, Dakar - Hann centre, 50 p.
11. Cheverry J. C. and Bourrie G. La salinisation des sols. "Sols C2 : interfaces fragiles". Part 3 : Consequences of human use of soils. 1995 ; Co-publication INRA/Nathan, 24 p.
12. Ould Mohamedou A, Aventurier A, Barbiéro L, Caruba R, Valles V. Geochemistry of Clay dunes and associated pan in the Senegal delta (Mauritania). 1999 ; Arid Soil Research Rehabilitation; 13: 265-80.
13. Barbiero L., Ould Mouhamedou A., Caruba R. Influence of mangrove soil maturation on aeolian deflation and clay dune formation in the Senegal River delta. 1998 ; Acad. Sci. Paris, Sciences de la terre et des planètes, 327 : 115 - 120.
14. Seiny-Boukar L. Les sols de la cuvette de Nder (lac de Guiers, Sénégal) : Caractéristiques et principaux aspects de leur mise en valeur agricole. 1983 ; In Problématique de l'environnement et du développement sahélien. University of Dakar (Senegal) ; pp 197-204.
15. Ould Mouhamedou A. Contribution à l'étude de l'environnement du parc national du Diawling (Mauritanie). 1998 ; Eaux - Sols - Végétation, Thesis, Université de Nice-Sophia Antipolis, 155 p.
16. Maymard J. Pedological studies in the alluvial valley of Senegal. 1960 ; MAS, Div. Agronomique, bull. 22.
17. Wind G. P. Capillary conductivity data estimated by a simple method. 1968 ; In : P.E. Rijtema and H. Wassink (editors), Water in the unsaturated zone, Proceedings of the Wageningen symposium, June 1966, IASH Gentbrugge/ Unesco Paris, vol. 1, pp. 181-191.
18. Van Genuchten M. Th., Leij F.J. and Yates S. R. The RETC code for Quantifying the Hydraulic Functions of Unsaturated Soils. 1991 ; U. S. Laboratory; U. S. Depertement of agricultural research service, Riverside, California 92501.
19. Marquardt, D. W. An algorithm for least-squares estimation of nonlinear parameters. 1963 ; J. Soc. Ind. Appl. Math. 11 : 431 - 441.
20. Hamdi Aissa B., Féodoroff N. and Valles V. Short and long term soit system behaviour in hyper-arid environment (a case study in the Ouargla Chott, Sahara of Algeria). 1997 ; in International Symposium Soit System Behaviour in Rime and Space, 19-21 November 1997, Vienna, Austria.
21. Ould Mohamedou A. Pedogenetic evolution of mangrove soils in the Senegal River valley and associated phenomena. 2000 ; Post-doctoral research report. Inra/Cirad/IRD/Aupelf-Uref; 30 p.
22. Vieillefon J. Sur l'existence de bourrelets éoliens ou lunettes dans les mangroves de Casamance. 1967 ; in : Actes du congrès panafricain de préhistoire, Dakar, 6ème session, Chambéry, 436-441.
23. Thomas, DSG, Nash, DJ, Shaw, PA and Van der Post, C. The current cycle of Witpan lunette sediments in the arid southwest Kalahari Desert. 1993 ; Catena, 20 (5), 515-527.
24. Dent D. Acid sulfate soils : a baseline for research and development. Wageningen. 1986 ; ILRI publication, 39 ; 200 p.
25. Barbiero L., Cunnac S., Mane L., Laperousaz C., Hammecher C. and Maeght J.L. Salt distribution in the Senegal River middle valley. Analysis of saline structure on the future irrigation scheme from Ngalenka. 2000 ; Creek, Agricultural Water Management.

COMPETING INTERESTS

Authors have declared that no competing interests exist.